Journal of Magnetism and Magnetic Materials 451 (2018) 620–624

Contents lists available at ScienceDirect

Journal of Magnetism and Magnetic Materials

journal homepage: www.elsevier.com/locate/jmmm

Research articles

On the magnetic properties of the multiferroic ceramics $Bi_{0.99}Y_{0.01}Fe_{1-x}Ni_xO_3$ $(0.01 \leqslant x \leqslant 0.05)$

D.R. Ratkovski [a], P.R.T. Ribeiro [a], F.L.A. Machado [a,*], P. Banerjee [b], A. Franco Jr. [c]

[a] Departamento de Física, Universidade Federal de Pernambuco, 50670-901 Recife, Pernambuco, Brazil
[b] Department of Physics, GITAM University, 561203 Bengaluru Rural District, Karnataka, India
[c] Instituto de Física, Universidade Federal de Goiás, 74690-900 Goiânia, Goiás, Brazil

ARTICLE INFO

Article history:
Received 15 April 2017
Received in revised form 15 September 2017
Accepted 24 November 2017
Available online 5 December 2017

Keywords:
Bismuth ferrite
Ionic doping
Magnetic properties

ABSTRACT

Multiferroic ceramics of $Bi_{0.99}Y_{0.01}Fe_{1-x}Ni_xO_3$ with $0.01 \leqslant x \leqslant 0.05$ were synthesized by using a modified solid state reaction method. The crystalline structure and the morphology of the samples were investigated by X-ray diffraction (XRD) and by scanning electron microscopy (SEM). The addition of Y and Ni to the bismuth ferrite ($BiFeO_3$) was found to decrease the average grain size. Ac magnetic susceptibility and the zero-field-cooled (ZFC) and field-cooled (FC) magnetizations were measured for temperatures in the range $5 \leqslant T \leqslant 300$ K. Hysteresis loops and an irreversible behavior in the temperature dependence of the magnetization not present in pure $BiFeO_3$ were observed in the doped samples. However, the ferromagnetism was found more likely to be due to the presence of small amounts of magnetite. Nevertheless, the determination of the amount of Fe_3O_4 in these composite materials is important because it influences the magnetoelectric coupling which is important for some technological applications.

1. Introduction

Single-phase (SP) multiferroic materials which exhibit noticeable magneto-electric (ME) coupling at room temperature (RT) have attracted a lot of attention in recent years due to their potential applications in multi-state memory and quantum controlling devices [1–3]. Bismuth ferrite ($BiFeO_3$) is one of the most investigated SP multiferroic material at RT. This material has a quite large difference between magnetic and ferroelectric transition temperatures, exhibiting antiferromagnetic order at a relatively high Néel temperature ($T_N \sim 643$ K) while a ferroelectric phase transition [4] occurs at 1098 K. The non-collinear G-type anti-ferromagnetic (AFM) ordering in $BiFeO_3$ (BFO) corresponds to the coupling of two adjacent crystal planes in the Fe^{3+} sites. The ferroelectric phase corresponds to the R3c space group symmetry with cations displaced from the $[111]_C$ direction with tilted oxygen octahedra [5]. Although the magnetic properties of BFO above RT have already been investigated [6] there are still considerable interest in investigating the magnetic properties at low temperatures. For instance, dc (χ_{dc}) and ac (χ_{ac}) magnetic susceptibilities measurements revealed that the magnetic moments in BFO varies little with temperature below RT [7,8]. However, intrinsic point defects such as oxygen vacancies in BFO sintered at high temperatures were found to influence the magnetic properties of this compound. It is also important to recall that there are already quite few studies reporting ferromagnetism in samples of BFO doped with different atomic elements [9–14]. For instance, while a Y-doping of about 1% was found to reduce the volatilization of Bi and oxygen vacancies [15], an enhancement of the ferromagnetic properties were observed in Ni-doped samples [16]. However, the ferromagnetic properties observed in these sample materials did not scale with the nominal doping concentration, raising a question whether the ferromagnetism is indeed intrinsic to the BFO phase.

In order to better clarify this point, $BiFeO_3$ and $Bi_{0.99}Y_{0.01}Fe_{1-x}Ni_xO_3$ $(0.01 \leqslant x \leq 0.05)$ (BYFN) poly-crystalline ceramics have been prepared by using a modified solid state reaction method. This method was found to produce this kind of ceramics with less oxygen vacancies because during the synthesis procedures the samples are kept at high temperatures for few minutes only. Our studies have been focused mainly on the effect of doping in the magnetic properties of these materials at low temperatures. As discussed below, it was found that the origin of the ferromagnetic phase is more likely to be due to the presence of traces of a secondary phase not detected by usual techniques used to characterize the structure and morphology of the sample materials.

* Corresponding author.
E-mail address: flam@df.ufpe.br (F.L.A. Machado).

https://doi.org/10.1016/j.jmmm.2017.11.103
0304-8853/

2. Experimental procedures

Policrystalline powder samples of $BiFeO_3$ and $Bi_{0.99}Y_{0.01}Fe_{1-x}Ni_xO_3$ with $0.01 \leqslant x \leqslant 0.05$ were prepared by a modified solid state reaction method [17]. High purity (99.9%) powders of Bi_2O_3, Fe_2O_3, Y_2O_3 and NiO were used in stoichiometric compositions as the sintering materials. The powders samples were sintered in a pre-heated muffle furnace at 1153 K for 20 min and leached with 10% diluted nitric acid at room temperature. The final power was then cold-isostatic pressed into 2 mm thick and 10 mm diameter pellets and the pellets were annealed at 1076 K for 15 min.

The samples were characterized by X-ray diffraction (XRD) by using the Cu – kα radiation. The dc magnetization measurements were carried out using the ACMS Modulus of a PPMS (Physical Properties Measurements System by Quantum Design) in zero-field-cooled (ZFC) and field cooled (FC) procedures from 5 K to 300 K for an applied magnetic field (H) of 500 Oe. In the ZFC procedure the samples were first cooled with $H = 0$, the magnetic field was then applied at 5 K and the magnetization measured in the heating up mode. For the field-cooled (FC) procedure, the samples were first cooled down to 5 K with $H = 500$ Oe and the magnetization was measured in the heating up as well. The measurement of the ac magnetic susceptibility was also carried out in the PPMS system using an ac magnetic field with, respectively, an amplitude and frequency of 10 Oe and 1 kHz for temperatures in the range 5 – 300 K.

3. Results and discussions

XRD spectra with their corresponding Rietveld refinements for pure BFO and doped BYFN ceramics are shown in Fig. 1. The XRD peak intensities showed that the polycrystalline samples present a good crystallinity. The diffraction peaks were indexed by using the rhombohedral perovskite (R3c space group, ICSD 86–1518) crystalline structure. Small traces of the ferrimagnetic Fe_3O_4 phase observed [18,19] in ceramics with similar sample compositions are also present in our samples. The position of the peak characteristics of this crystalline phase is indicated in the XRD spectra by an asterisks. Despite of the intensities of the XRD peak the Fe_3O_4 be almost undetectable we found that small amounts of this phase influenced drastically the overall magnetic data. However, the mullite $Bi_2Fe_4O_9$ phase [20,21] characterized by a peak near the angle $2\theta = 28$ degrees is not observed in the samples investigated in the present work. The incorporation of Y^{3+} with smaller ionic radius than Bi^{3+} distorces the rhombohedral structure. The effect of the ionic doping in the perovskite structure of the BFO can be accounted by taking into consideration the Goldschmidt tolerance factor [22]:

$$t = \frac{\left[(1-y)r_{Bi^{3+}} + yr_{Y^{3+}} + r_{O^{2-}}\right]}{\sqrt{2}\left[(1-x)r_{Fe^{3+}} + xr_{Ni^{2+}} + r_{O^{2-}}\right]}, \quad (1)$$

where $r_{Bi^{3+}}$ and $r_{Y^{3+}}$ are the twelve-fold co-ordination ionic radii of Bi^{3+} and Y^{3+} and $r_{Fe^{3+}}$, $r_{Ni^{2+}}$ and $r_{O^{2-}}$ are the sixfold coordination ionic radii of Fe^{+3}, Ni^{+2} and O^{+2} ions, respectively. The tolerance factor decreased from the 0.939 for the BFO to the 0.937 for the BYFN ceramics with $x = 0.05$ because of the distortion of the FeO_6 octahedra. Rietveld analysis was employed to the XRD data for determining the lattice parameters a and c, average crystallite sizes d and the mass density ρ associated to the BFO crystalline structure. d was found to be the most influenced parameters for the concentration range used in the present work. These results are summarized in Table 1.

Fig. 2 show SEM images for pure BFO (a) and for the BYFN 2 (b) ceramics for a magnification factor of 1kx. The corresponding insets are images from the same samples magnified by a factor ten times larger where one can clearly see that the doping process decreases the overall grain size. This effect has been attributed to a

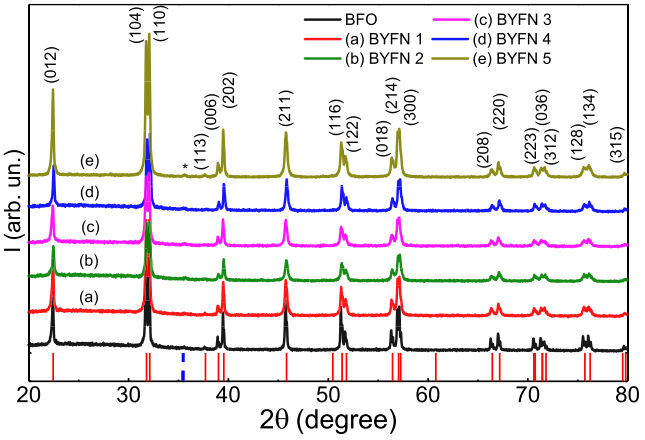

Fig. 1. Room temperature X-ray diffraction patterns of pure BFO and doped BYFN powders. The asterisk (*) marks the presence of a peak that it is characteristic of the Fe_3O_4 phase.

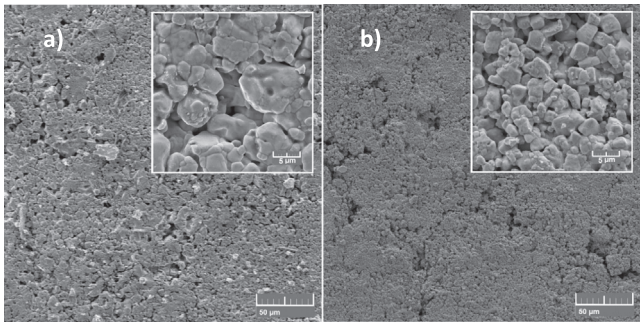

Fig. 2. SEM images for the fracture surface of (a) BFO and (b) BYFN-2 obtained with a magnification of 1kx while the correponding insets were obtained with magnification of 10kx.

Table 1
Structural data obtained by using the Rietveld analysis.

Sample	Cell parameters		Density	Crystallite size	Reliability
	a (nm)	c (nm)	ρ (g/cm^3)	d (nm)	χ^2
BFO	0.5567	1.3838	8.962	218.00	1.651
BYFN 1	0.5575	1.3856	8.476	119.57	1.703
BYFN 2	0.5578	1.3861	8.477	111.71	1.573
BYFN 3	0.5578	1.3860	8.348	99.99	1.672
BYFN 4	0.5540	1.3770	8.692	152.41	1.295
BYFN 5	0.5568	1.3837	8.998	94.16	1.595

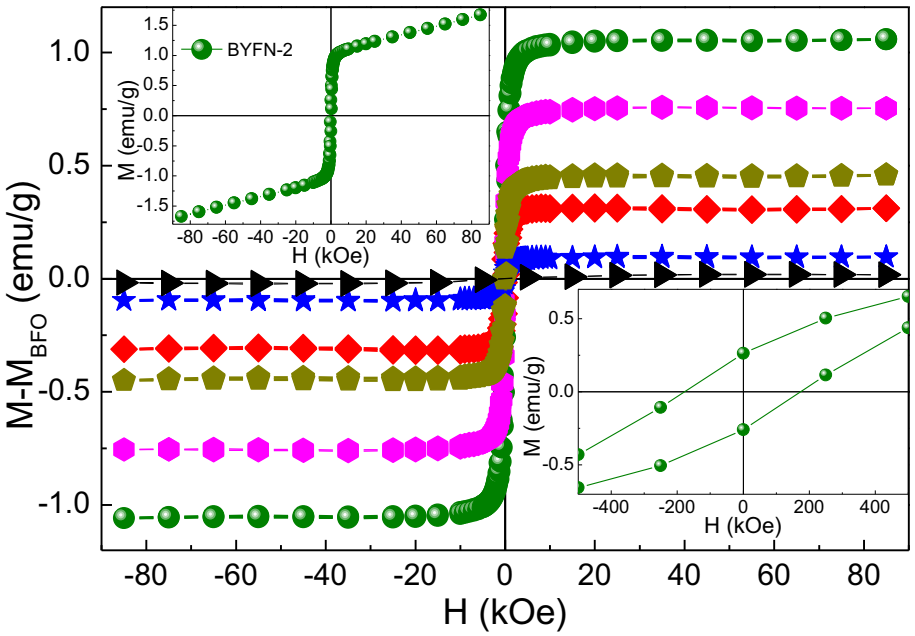

Fig. 3. Magnetization minus the AFM contribution of pure BFO measured at 5 K for $x = 0$ (triangles), 0.01 (diamonds), 0.02 (circles), 0.03 (hexagons), 0.04 (stars) and 0.05 (pentagons). A full hysteresis loop is shown in the upper left inset for $x = 0.02$ while a blow-up of this histeresis loop is shown in the lower left inset. The net magnetization shows histeresis loops for all values of the Ni concentration but the data in the high applied magnetic field regime do not scale with x. The solid lines are guides to the eyes.

pinning effect that decreases the ionic mobility across the grain boundaries [23].

Ferromagnetic hysteresis loops superimposed to a contribution proportional to H that extended up to the highest applied magnetic field (=85 kOe) were observed for all doped samples and for three values of temperature: 5, 150 and 300 K. The contribution proportional to H is actually the one expected for the antiferromagnetic phase of BFO. A typical M versus H curve is shown in the inset of Fig. 3 for the sample which presented the largest ferromagnetic contribution ($x = 0.02$) measured at $T = 5$ K. However, it was noticed that the amount of the ferromagnetic phase did not scale with Ni-doping. Thus, the BFO linear contribution $M_{BFO} = \chi_{BFO}H$, where $\chi_{BFO} = 7.83 \times 10^{-6}, 6.84 \times 10^{-6}$ and 6.27×10^{-6} emu/g for $T = 5, 150$ and 300 K, respectively, was subtracted from the overall magnetization data yielding the hysteresis loops shown in Fig. 5. It was also noticed that for the sample with $x = 0.02$ the room temperature coercivity ($H_c = 138$ Oe) and the ratio of the remanent to the saturation magnetization ($M_r/M_s = 0.21$) were closer to the values obtained for magnetites [24], e.g., $H_c = 138$ Oe and

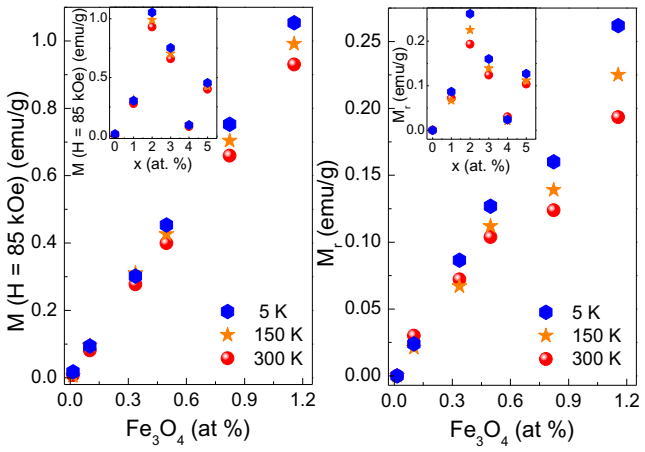

Fig. 4. Magnetization measured at the highest applied magnetic field $M(H = 85$ kOe) (left) and remanence M_r (right) versus the concentration of Fe_3O_4. M_r and $M(H = 85$ kOe) were found to scale with the amount of magnetite for $T = 5, 150$ and 300 K. The insets show that the data become scattered when they are plotted versus the Ni concentration.

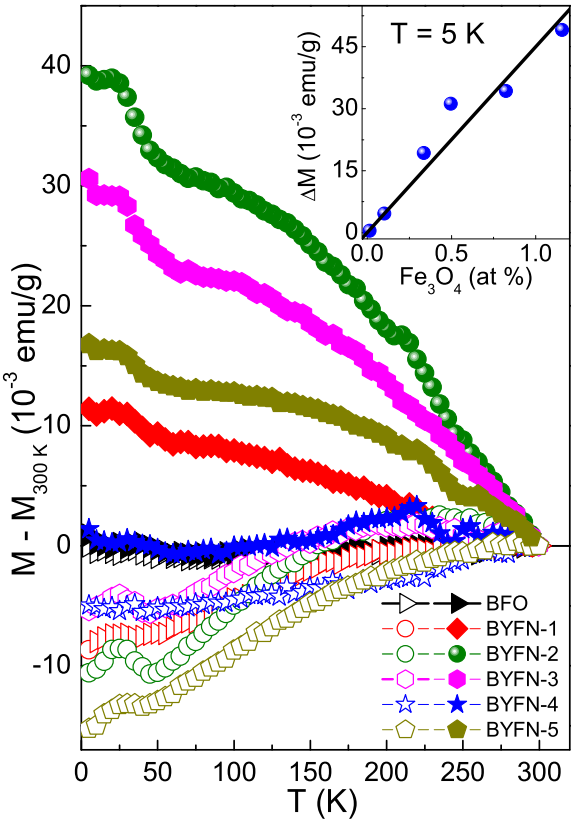

Fig. 5. T-dependence for the ZFC and FC magnetizations minus the corresponding values measured at 300 K for $H = 500$ Oe. The size of the irreversibility does not scale with x. Instead, it scales with the relative amount of Fe_3O_4 as shown in the inset for $T = 5$ K. The solid line is a guide to the eyes.

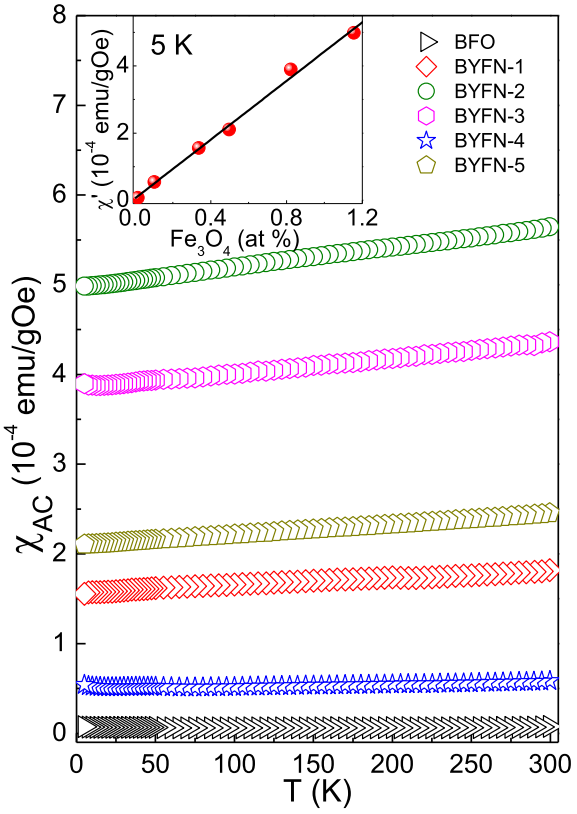

Fig. 6. *T*-dependence for χ_{ac} measured by using an ac magnetic field with amplitude of 10 Oe and frequency of 1 kHz. χ_{ac} does not also scale with x but with relative amount of Fe_3O_4 as shown in the inset for $T = 5$ K. The solid line is a guide to the eyes.

$M_r/M_s = 0.22$. Thus, to verify that the ferromagnetism present in the doped samples was indeed not intrinsic to the doped BFO samples, it was estimated the fraction of Fe_3O_4 that would be required for yielding the values obtained for the magnetization measured at 300 K for the highest applied magnetic field $M(H = 85$ kOe) by using $M_s = 89.2$ emu/g [24]. For instance, for the sample with $x = 0.02$ it would be required about 1.2% ($\approx 100 \times 1.05/89.2$) of magnetite to yield a hysteresis loop similar to the one obtained for this sample composition. Using the same procedure for the other samples it was found that the corresponding amounts of magnetite (with corresponding Ni-doping) were: 0.34% ($x = 0.01$); 1.2% ($x = 0.02$), 0.82% ($x = 0.03$), 0.1% ($x = 0.04$), 0.5% ($x = 0.05$). It is interesting to mention that the concentration of Fe_3O_4 determined from the hysteresis measured at 300 K ordered both $M(H = 85$ kOe) and M_r data at 5, 150 K and 300 K as shown in Fig. 4.

In order to verify that the correlation of the hysteresis loops with the amount of Fe_3O_4 was not a fortuity one, the ZFC and FC magnetizations were measured for all samples for $H = 500$ Oe. The results are shown in Fig. 5. The room temperature magnetization data was actually subtracted from the ZFC and FC magnetizations for magnifying the irreversible behavior. Again, it was not observed a correlation in the magnitude of irreversibility with the Ni concentration in the same manner as for the hysteresis loops. However, if it is used the concentrations of Fe_3O_4 as determined above, one finds a reasonably good correlation as shown in the inset of Fig. 5. The correlation is actually represented in the plot of the difference between the ZFC and FC magnetizations data ($= \Delta M$) measured at 5 K. The characteristic temperature associated to the irreversibility was found to be above room temperature.

The correlation of the magnetic data with the concentrations of Fe_3O_4 was also tested for a very low value of applied magnetic field by measuring the magnitude of the ac magnetic susceptibility $\chi_{AC} = \sqrt{\chi_R^2 + \chi_I^2}$, where χ_R and χ_I are the in-phase and out-of-phase components of χ_{AC}, respectively, for a frequency of 1 kHz, magnitude of the ac magnetic field of 10 Oe and temperatures in the range 5–300 K. These results are shown in Fig. 6. The inset of Fig. 6 shows the χ_{AC} data for $T = 5$ K. It is also seen that the data is also nicely correlated with the concentration of Fe_3O_4 and not with the Ni concentration. Small amounts of Fe_3O_4 can be expected to be present into $Bi_{0.99}Y_{0.01}Fe_{1-x}Ni_xO_3$ due to the uncertainties inherent in obtaining the stoichometry necessary to produce these materials, e.g., unreacted iron may easily oxidize yielding the magnetite phase.

4. Conclusions

In summary, a series of $Bi_{0.99}Y_{0.01}Fe_{1-x}Ni_xO_3$ and $BiFeO_3$ ceramic samples were synthesized using a modified solid state reaction method and their magnetic properties were carefully investigated. A ferromagnetic phase indicated by a superposition of hysteresis loops to the antiferromagnetic contribution characteristic of BFO was observed for all doped samples. Despite the XRD and SEM data do not allow one to identify the presence of small amounts of spurious phase, the magnetic analyzes indicated that the ferromagnetic phase is more likely be associated to traces of magnetite (Fe_3O_4) present in the doped samples. For instance, one of the samples with the highest concentration of Ni ($x = 0.04$) was the one showing less magnetite ($= 0.01\%$) and with the overall magnetic data closer to the ones of BFO. The amount of Fe_3O_4 was estimated from the magnetization data measured at room temperature for the highest applied magnetic field ($H = 85$ kOe). By using the concentration of Fe_3O_4 it was possible to correlate well all the magnetic data with this sample parameter. The results presented in the current work yielded a clue of why some of the data reported in the literature shows doped samples that are ferromagnetic and other that are not. The magnetic analysis used in the current work seems to be a good method for analyzing samples with small amounts of ferromagnetic phases that are hardly detected by conventional characterization techniques. Moreover, it was shown that higher magnetic fields than the ones currently used are required for separating the antiferromagnetic contribution from ferromagnetic magnetic phase. Regardless the ferromagnetic phase be intrinsic or not, it influences the magnetoelectric coupling which, in turn, it is important for technological applications.

Acknowledgements

This work was partially supported by CNPq, CAPES, FINEP, FACEPE and FAPEG (Brazilian Agencies).

References

[1] M. Fiebig, Revival of the magnetoelectric effect, J. Phys. D: Appl. Phys. 38 (2005) R123, https://doi.org/10.1088/0022-3727/38/8/R01.
[2] W. Eerenstein, N.D. Mathur, J.F. Scott, Multiferroic and magnetoelectric materials, Nature 442 (2006) 759, https://doi.org/10.1038/nature05023.
[3] N.A. Spaldin, S.-W. Cheong, R. Ramesh, Multiferroics: past, present, and future, Phys. Today 63 (2010) 38, https://doi.org/10.1063/1.3502547.
[4] I. Sosnowska, T.P. Neumaier, E. Steichele, Spiral magnetic ordering in bismuth ferrite, J. Phys. C Solid State 15 (1982) 4835, https://doi.org/10.1088/0022-3719/15/23/020.
[5] X. Qingyu, W. Zheng, G. Jinlong, W. Di, T. Shaolong, X. Mingxiang, The multiferroic properties of $Bi(Fe_{0.95}Co_{0.05})O_3$ films, Physica B 406 (2011) 2025, https://doi.org/10.1016/j.physb.2011.03.011.
[6] G. Catalan, J.F. Scott, Physics and applications of bismuth ferrite, Adv. Mater. 21 (2009) 2463–2485, https://doi.org/10.1002/adma.200802849.

[7] S. Nakamura, S. Soeya, N. Ikeda, M. Tanaka, Spin-glass behavior in amorphous $BiFeO_3$, J. Appl. Phys. 74 (9) (1993) 5652, https://doi.org/10.1063/1.2711279.
[8] H. Naganuma, S. Okamura, Structural, magnetic, and ferroelectric properties of multiferroic $BiFeO_3$ film fabricated by chemical solution deposition, J. Appl. Phys. 101 (2007) 9M103, https://doi.org/10.1063/1.354179.
[9] Y. Wang, G. Xu, L. Yang, Z. Ren, X. Wei, W. Weng, P. Du, G. Shen, G. Han, Enhancement of ferromagnetic properties in Ni-doped $BiFeO_3$, Mater. Sci.-Poland 27 (2009) 219.
[10] Y.A. Chaudhari, C.M. Mahajan, P.P. Jagtap, S.T. Bendre, Structural, magnetic and dielectric properties of nano-crystalline Ni-doped $BiFeO_3$ ceramics formulated by self-propagating high-temperature synthesis, J. Adv. Ceramics 2 (2013) 135, https://doi.org/10.1007/s40145-013-0051-3.
[11] Y. Chaudhari, A. Singhm, C.M. Mahajan, P. Jagtap, E.M. Abuassaj, R. Chatterjee, S.T. Bendre, Multiferroic properties in Zn and Ni co-doped $BiFeO_3$ ceramics by solution combustion method (SCM), J. Magn. Magn. Mater. 347 (2013) 153, https://doi.org/10.1016/j.jmmm.2013.08.003.
[12] V. Singh, S. Sharma, R.K. Dwivedi, M. Kumar, R.K. Kotnala, N.C. Mehra, R.P. Tandon, Structural, dielectric, ferroelectric and magnetic properties of $Bi_{0.80}A_{0.20}FeO_3$ (A=Pr, Y) multiferroics, J. Supercond. Nov Magn. 26 (3) (2013) 657, https://doi.org/10.1007/s10948-012-1775-y.
[13] D. Kuang, P. Tang, X. Ding, S. Yang, Y. Zhang, Effects of y doping on multiferroic properties of sol gel deposited $BiFeO_3$ thin films, J. Mater. Sci.-Mater. El. 26 (2015) 3001, https://doi.org/10.1016/j.materresbull.2016.01.018.
[14] N.I. Ilic, J.D. Bobic, B.S. Stojadinovic, A.S. Dzunuzovic, M.M.V. Petrovic, Z.D. Dohcevic-Mitrovic, B.D. Stojanovic, Improving of the electrical and magnetic properties of $BiFeO_3$ by doping with yttrium, Mater. Res. Bull. 77 (2016) 60, https://doi.org/10.1007/s10854-016-4530-5.
[15] A. Mukherjee, M. Banerjee, S. Basu, N.T.K. Thanh, L. Green, M. Pal, Enhanced magnetic and electrical properties of Y and Mn co-doped $BiFeO_3$ nanoparticles, Physica B: Condensed Matter 448 (2014) 199, https://doi.org/10.1016/j.physb.2014.03.082.
[16] Y. Dai, Q. Xu, X. Zheng, S. Yuan, Y. Zhai, M. Xu, Magnetic properties of Ni-substituted $BiFeO_3$, Physica B: Condensed Matter 407 (2012) 560, https://doi.org/10.1016/j.physb.2011.11.055.
[17] P. Banerjee, A.J. Franco, Rare earth and transition metal doped $BiFeO_3$ ceramics: structural, magnetic and dielectric characterization, J. Mater. Sci.-Mater. El. 27 (6) (2016) 6053, https://doi.org/10.1007/s10854-017-6579-1.
[18] H. Bea, M. Bibes, A. Barthélémy, K. Bouzehouane, E. Jacquet, A. Khodan, J.P. Contour, S. Fusil, F. Wyczisk, A. Forget, D. Lebeugle, D. Colson, M. Viret, Influence of parasitic phases on the properties of $BiFeO_3$ epitaxial thin films, Appl. Phys. Lett. 87 (2005) 072508, https://doi.org/10.1063/1.2009808.
[19] M. Murakami, S. Fujino, S. Lim, L. Salamanca-Riba, M. Wuttig, I. Takeuchi, B. Varughese, H. Sugaya, T. Hasegawa, S. Lofland, Microstructure and phase control in Bi-Fe-O multiferroic nanocomposite thin films, Appl. Phys. Lett. 88 (11) (2006) 112505, https://doi.org/10.1063/1.2184892.
[20] K.G. Yang, Y.L. Zhang, S.H. Yang, B. Wang, Structural, electrical, and magnetic properties of multiferroic $Bi_{1-x}La_xFe_{1-y}Co_yO_3$ thin films, J. Appl. Phys. 107 (2010) 124109, https://doi.org/10.1063/1.3437232.
[21] P. Kumar, M. Kar, Tuning of net magnetic moment in $BiFeO_3$ multiferroics by co-substitution of Nd and Mn, Physica B 448 (2014) 90, https://doi.org/10.1016/j.physb.2014.03.080.
[22] V. Goldschmidt, Die gesetze der krystallochemie, Naturwissenschaften 14 (1926) 477, https://doi.org/10.1007/BF01507527.
[23] T.D. Berman, T.M. Pollock, J.W. Jones, Microstructure and texture through thixomolding and thermomechanical processing and the role of Mg17Al12 particles, Metall. Mater. Trans. A 47 (6) (2016) 3125, https://doi.org/10.1007/s11661-016-3450-6.
[24] O. Ozdemir, D.J. Dunlop, B.M. Moskowitz, Changes in remanence, coercivity and domain state at low temperature in magnetite, Earth Planet. Sc. Lett. 194 (2002) 343, https://doi.org/10.1016/S0012-821X(01)00562-3.